Gyrokinetic particle simulation of beta-induced Alfven-acoustic eigenmode

H. S. Zhang,[1,2,a)] Y. Q. Liu,[1] Z. Lin,[3] and W. L. Zhang[4]

[1]*Fusion Simulation Center, Peking University, Beijing 100871, China*
[2]*Institute of Applied Physics and Computational Mathematics, Beijing 100088, China*
[3]*Department of Physics and Astronomy, University of California, Irvine, California 92697, USA*
[4]*Institute of Physics, Chinese Academy of Sciences, Beijing 100190, China*

The beta-induced Alfven-acoustic eigenmode (BAAE) in toroidal plasmas is verified and studied by global gyrokinetic particle simulations. When ion temperature is much lower than electron temperature, the existence of the weakly damped BAAE is verified in the simulations using initial perturbation, antenna excitation, and energetic particle excitation, respectively. When the ion temperature is comparable to the electron temperature, the unstable BAAE can be excited by realistic energetic particle density gradient, even though the stable BAAE (in the absence of energetic particles) is heavily damped by the thermal ions. In the simulations with reversed magnetic shear, BAAE frequency sweeping is observed and poloidal mode structure has a triangle shape with a poloidal direction similar to that observed in tokamak experiments. The triangle shape changes the poloidal direction, and no frequency sweeping is found in the simulations with normal magnetic shear. *Published by AIP Publishing.*
[http://dx.doi.org/10.1063/1.4947205]

I. INTRODUCTION

The Alfven eigenmodes,[1,2] such as the beta-induced Alfven eigenmode (BAE),[3,4] reversed shear Alfven eigenmode (RSAE),[5,6] and beta-induced Alfven-acoustic eigenmode (BAAE),[7,8] have attracted significant attention in recent tokamak studies. These modes can cause the loss of energetic particles and are deleterious to the plasma performance. Since the BAAE frequency is dependent on the safety factor in the tokamaks, it can also be used for the diagnosis of the safety factor. The BAAE has been observed in various tokamaks such as JET, NSTX, and DIII-D.[8,9]

The BAAE is formed through the coupling of the shear Alfven continuum and the acoustic continuum in the toroidal geometry, which was first formulated based on magnetohydrodynamic (MHD) approach.[7,8] As shown in Ref. 9, the theoretical BAAE dispersion relation in the MHD limit can be estimated as $\omega_{BAAE} = V_A k_{//}/\sqrt{1+2q^2}$. The frequency of BAAE is much lower than the frequency of BAE or RSAE, since the BAAE gap is under the gap of BAE or RSAE in the Alfven continuum. Due to its low frequency, the BAAE can be strongly damped by thermal ions when ion temperature (T_i) and electron temperature (T_e) are comparable. Therefore, it has been debated whether the BAAE as predicted by the MHD theory could exist in the collisionless plasmas of fusion interest where BAAE is expected to be heavily damped by ion kinetic effects.[10–12] A kinetic approach is thus required for the accurate simulation of the BAAE. In this work, the BAAE is verified and studied through global gyrokinetic particle simulations for the first time using the gyrokinetic toroidal code (GTC).[13–15] GTC has been successfully applied to the kinetic study of the low

frequency MHD modes such as geodesic acoustic mode (GAM),[16,17] BAE,[18–20] RSAE,[21] toroidal Alfven eigenmode (TAE),[22–24] energetic particle mode (EPM),[25] as well as current-driven MHD instabilities including internal kink mode[26] and resistive tearing mode.[27]

In the current work, the existence of BAAE is first verified when ion temperature is much smaller than electron temperature ($T_i \ll T_e$) in the GTC simulations using initial perturbation, antenna excitation, and energetic particle excitation, separately. It is found that the BAAE is weakly damped when $T_i \ll T_e$. The BAAE frequency excited by the antenna and energetic particles is almost the same as that in the initial perturbation simulation. The linear BAAE properties with $T_i = 0.5T_e$ are then studied in the GTC simulations for both reversed shear and monotonic q profiles. It is shown in the antenna excitation simulations that the damping rate of the BAAE is comparable to its real frequency when T_i and T_e are comparable. However, the BAAE can still be excited by a modest energetic particle density gradient with a frequency slightly higher than that estimated from the antenna excitation. The simulations find that BAAE mode structure in the reverse magnetic shear is similar to that observed in the DIII-D experiments.[28] The BAAE poloidal mode structure in the normal magnetic shear has opposite triangle eddy shape compared to that in the reversed shear. Furthermore, BAAE frequency sweeping is observed in the reversed shear, consistent with the experimental observations.[9] No frequency sweeping is found in the normal shear simulation. The frequency of the unstable BAAE is slightly higher than the prediction of the MHD theory.

The paper is organized as follows: The verification of the existence of BAAE in the $T_i \ll T_e$ limit is presented in Sec. II. In Sec. III, the linear BAAE properties with $T_i = 0.5T_e$ are studied. Section IV is the summary.

a)Author to whom correspondence should be addressed. Electronic mail:
zhang.huasen@gmail.com

II. VERIFICATION OF BAAE IN $T_i \ll T_e$ LIMIT

The GTC simulations use a tokamak with a major radius $R_0 = 4$m and a minor radius $a = 0.3R_0$. The concentric circular toroidal magnetic field is used with an on-axis magnetic field $B_0 = 3.82$T. Protons are used as the background ions with a uniform temperature. The electron temperature and density are uniform with $T_e = 4500$eV, $n_e = 1.3 \times 10^{14}(\text{cm}^{-3})$, and $\beta_e = 4\pi n_0(T_e)/B_0^2 = 2.87\%$. The ions are treated using the gyrokinetic equations, while the electrons are treated as a massless fluid[14] in the current simulations. A safety factor (q) profile with a reversed shear is used with $q_{min} = 1.48$ locates at $\epsilon = r/R_0 = 0.15$ (r is the local minor radius) (Fig. 1). The n = 4 mode is selected in the linear simulation. Since the BAAE is a $k_{//} \approx 0$ mode, we further apply a poloidal harmonic filter to keep only the $m \in [nq - 2, nq + 2]$ harmonics to avoid the high frequency noise. The wavelength of the BAAE is $k_\theta \rho_i = 0.01$, and 32 grid points per wavelength are used in the simulation.

Since the BAAE can be strongly damped by the thermal ions due to its low frequency, it is easier to excite in the $T_i \ll T_e$ limit. In this case, the BAAE frequency can be much larger than the thermal ion transit frequency and thus is only weakly damped by the thermal ions. We first search the BAAE with $T_i = 0.02T_e$ in our simulations using the initial perturbation, antenna excitation, and energetic particle excitation, separately. In the initial perturbation simulation, a harmonic of (n,m) = (4,6) electron density perturbation is initiated around the q_{min} surface and evolves self-consistently. Figure 2(a) shows the time evolution of the electrostatic potential for the (4,6) harmonic. The frequency spectrum of the (4, 6) harmonic (Fig. 2(b)) shows that it consists of two frequencies with almost the same intensity. The higher frequency $\omega \approx 0.105V_A/R_0$ (V_A is the Alfven speed) corresponds to the RSAE, while the lower frequency $\omega \approx 0.047V_A/R_0$ corresponds to the BAAE. The initial perturbation simulation shows that both RSAE and BAAE can be observed around the q_{min} surface in the $T_i \ll T_e$ limit. In order to further investigate the BAAE properties, we first perform fast Fourier transform in time for the electrostatic potential of the (4,6) harmonic and keep only the lower frequency component in the frequency spectrum (indicated by the black curve in Fig. 2(b)). Then, the frequency spectrum is transformed back to the time space. Now the (4,6) harmonic exhibits very good oscillation patterns with a
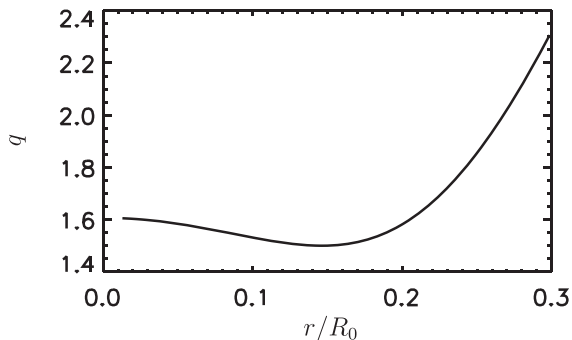
single frequency (Fig. 2(c)). It has a real frequency of $\omega = 0.047V_A/R_0$ and a finite damping rate of $\gamma = -0.0012V_A/R_0$, i.e., $\gamma/\omega = 2.5\%$. The damping rate is about 2.5% of the real frequency, indicating that the BAAE is weakly damped in the $T_i \ll T_e$ limit. Since the Landau damping of the BAAE is quite similar to that of the ion acoustic wave (IAW), the Landau damping rate of the BAAE can be approximately estimated from the Landau damping rate of the IAW. It is found that $\gamma_{ia}/\omega_{ia} = 1.4\%$ for IAW with $T_i = 0.02T_e$ (ω_{ia} and γ_{ia} are the real frequency and damping rate of the IAW, respectively).

Next, the BAAE is excited by an artificial antenna in GTC simulations.[17] A scan of the antenna frequency is used to verify the BAAE frequency and damping rate obtained in the simulation with initial perturbations. Similar method has already been successfully used in tokamak experiments and simulations.[17,29] Figure 2(d) shows the saturated BAAE amplitudes as a function of the antenna frequency (ω_{ant}). It is shown that the maximal saturated BAAE amplitude locates around $\omega = 0.048V_A/R_0$. According to the driven-resonant cavity theory,[30] the frequency and damping rate of the BAAE can be determined by the following equation:

$$A^2 \propto \frac{1}{(\omega_0^2 + \gamma^2 - \omega_{ant}^2 + 4\gamma^2\omega_{ant}^2)}. \quad (1)$$

Here, A^2 is the normalized saturated mode amplitude. ω_0 and γ are the real frequency and damping rate of the eigenmode, respectively. The numerical fitting of the simulation results shows that the real frequency and damping rate of the BAAE are $\omega = 0.048V_A/R_0$ and $\gamma = -0.0027V_A/R_0$, respectively. The BAAE frequency is quite close to the frequency obtained from the initial perturbation simulation. However, the damping rate is about twice higher than that obtained from the initial perturbation simulation. It should be noted that the estimation of the BAAE damping rate from the antenna frequency scan may not be as accurate as the initial perturbation for the very weakly damped mode, because it is difficult to reach a truly saturated mode amplitude in the simulations.

Finally, the energetic particle density gradient is used to excite the BAAE in the GTC simulations. The protons are used as the energetic particles with a maximum density gradient $R/L_{nf} \approx 12$ located at the q_{min} surface. The energetic particles have a Maxwellian distribution with $T_f = 9T_e$ and $n_f = 0.15n_e$, respectively. Figure 2(e) shows the time evolution of the (4,6) harmonic. This mode grows exponentially with a frequency $\omega = 0.048V_A/R_0$ and a growth rate $\gamma = 0.0076V_A/R_0$. The mode frequency agrees with the BAAE frequency observed in the initial perturbation and antenna excitation, indicating that the non-perturbative contribution of energetic particles has little effects on the BAAE frequency in the $T_i \ll T_e$ limit. It is also shown that the wave is a traveling wave and propagates in the fast ion diamagnetic direction. The radial mode structures of the electrostatic potential ϕ and vector potential $A_{||}$ are shown in Figs. 2(f) and 2(g), respectively. It is shown that the m = 6 harmonic is dominant around the mode rational surface in both ϕ and $A_{||}$. The amplitude of the m = 5 and m = 7

FIG. 1. Safety factor (q) profile used in the simulation.
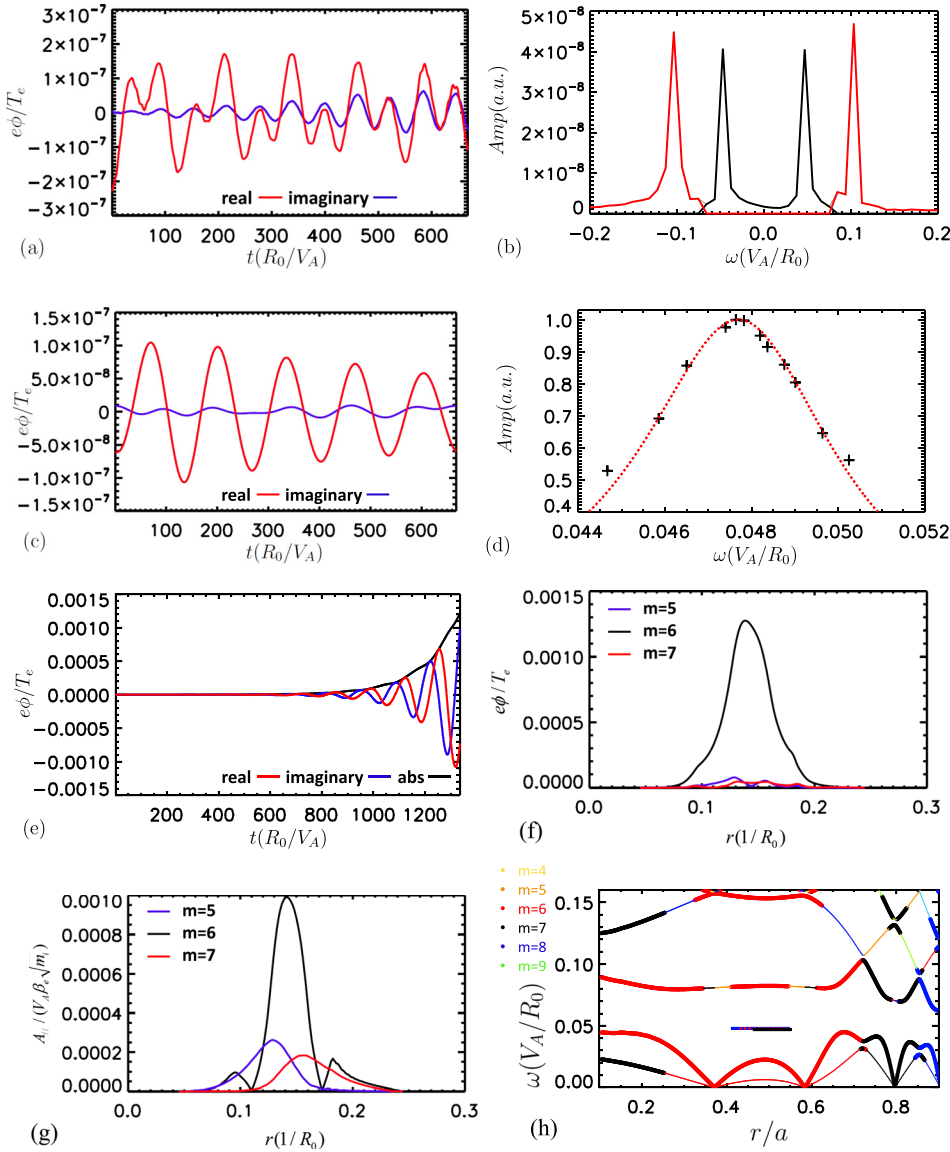
FIG. 2. Panels (a) and (b) are the amplitude evolution and frequency spectrum in the initial perturbation simulation. Panel (c) is the amplitude evolution of the BAAE obtained by keeping only the black curve in panel (b). Panel (d) is the saturated BAAE mode amplitude in the antenna frequency scan. The symbols in panel (d) are the simulation results and the red dotted curve is the numerical fitting. Panel (e) is the amplitude evolution in the energetic particle excitation simulation. Panel (f) and (g) are the radial mode structure of ϕ and $A_{\parallel}$, respectively. Panel (h) is the Alfven continuum for n = 4. The thick lines are the Alfven branches and the thin lines are the sound branches. The horizontal lines indicate the BAAE frequencies and mode width from the initial perturbation (solid black), antenna excitation (dashed red), and energetic particle excitation (solid blue). In panels (a), (c), and (e), the red and blue lines are the real part and imaginary part, respectively, and the black lines are the absolute value of the harmonic.

harmonics is relatively larger for $A_{\parallel}$ than that of ϕ compared to the m = 6 harmonic. Figure 2(h) shows the Alfven continuum for the equilibrium parameters. We can see that the BAAE gap is formed around $\omega = 0.06 V_A/R_0$. The BAAE frequencies obtained from the initial perturbation, antenna excitation, and energetic particle excitation are all very close to each other and locate well inside the BAAE gap.

III. LINEAR BAAE PROPERTIES WITH $T_i = 0.5 T_e$

In Sec. II, the BAAE is verified in the reversed shear plasma and in the $T_i \ll T_e$ limit. However, T_i and T_e are usually comparable in the tokamak experiments. In this regime, the kinetic effect could be crucial to the BAAE excitation, and the BAAE can be strongly suppressed by the thermal ions due to the significant Landau damping.[10] Furthermore, the linear BAAE properties may be different between the reversed and normal shear profiles. In order to investigate the linear BAAE properties when T_i and T_e are comparable, the GTC simulations with $T_i = 0.5 T_e$ are carried out in this section.

A. BAAE simulation with reversed shear q profile

In this section, the simulation parameters are the same as the simulation in Sec. II except for $T_i = 0.5 T_e$. Figure 3(a) is the frequency spectrum of the (4,6) harmonic in the initial perturbation simulation. The BAAE component is much smaller than the RSAE component due to the significant Landau damping of the BAAE when T_i and T_e are comparable. The real frequency of the BAAE is $\omega \approx 0.034 V_A/R_0$, while the damping rate is difficult to estimate. Figure 3(b) shows the saturated mode amplitude in the antenna frequency scan. The numerical fitting of the simulation results shows that the frequency and damping rate of the BAAE are $\omega = 0.037 V_A/R_0$ and $\gamma = -0.019 V_A/R_0$, respectively. The real frequency is very close to the BAAE frequency estimated from the initial perturbation. The damping rate is about 50% of the real frequency, indicating that the BAAE is strongly damped by the thermal ions. It is shown that the numerical fitting of the saturated BAAE amplitude is significantly deviated from the simulation results. Since the BAAE damping rate is comparable to the real frequency, this heavily damped mode probably cannot be accurately modeled by
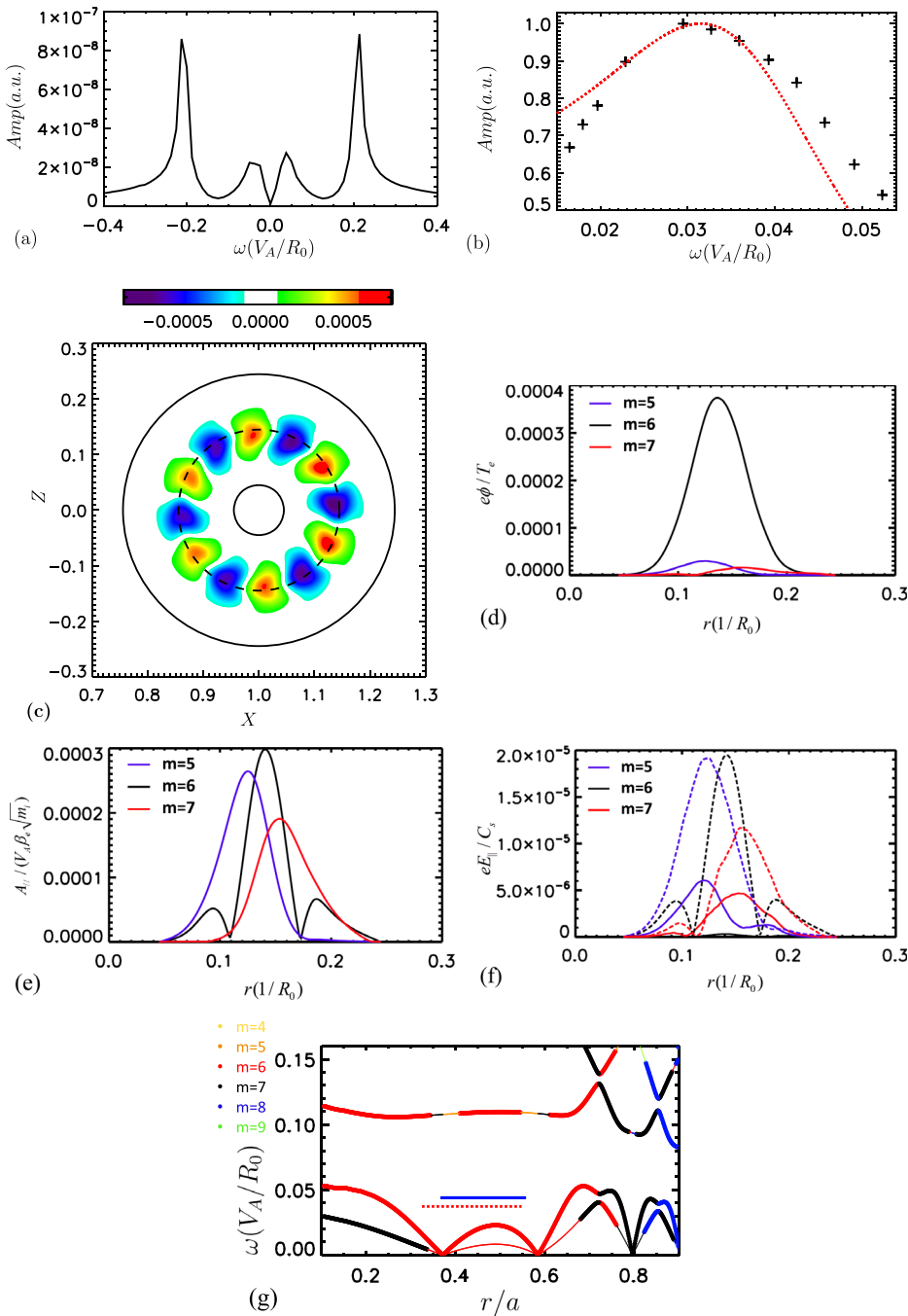
FIG. 3. Panel (a) is the frequency spectrum from simulations with initial perturbations. Panel (b) is the saturated BAAE mode amplitude in the antenna frequency scan. The symbols in panel (b) are the simulation results and the red dotted curve is the numerical fitting using Eq. (1). Panel (c) is the poloidal mode structure in the energetic particle simulation. Panels (d) and (e) are the radial mode structure of ϕ and $A_{||}$, respectively. Panel (f) is the radial mode structure of the parallel electric field calculated from ϕ_{eff} (solid) and ϕ (dash). Panel (g) is the Alfven continuum. The thick lines are the Alfven branches and the thin lines are the sound branches. The horizontal lines indicate the BAAE frequencies and mode width from the antenna excitation (dashed red) and energetic particle excitation (solid blue).

the driven-resonant cavity theory. In the energetic particle excitation simulation, the energetic particle temperature, density, and density gradient are $T_f = 9T_e$, $n_f = 0.1n_e$, and $R/L_{nf} \approx 12$, respectively. The unstable BAAE grows exponentially similar to Fig. 2(e). The BAAE frequency and growth rate are $\omega = 0.044 V_A/R_0$ and $\gamma = 0.019 V_A/R_0$, respectively. This frequency is slightly higher than the estimation from the initial perturbation and antenna excitation, which is probably due to the non-perturbative contribution of the energetic particles. The poloidal mode structure of the BAAE in the energetic particle excitation simulation is shown in Fig. 3(c). The m = 6 harmonic forms triangle shape around the q_{min} surface, i.e., a radial shearing of the eigenmode. We note that the clockwise direction of the triangle shape agrees with the BAAE mode structure measured in the

DIII-D experiments.[28] Similar structures are also observed in other energetic particle excited Alfven eigenmodes, such as TAE,[23] RSAE,[31] and BAE.[18] Figures 3(d) and 3(e) show the radial mode structures of the electrostatic potential ϕ and the vector potential $A_{||}$, respectively. The m = 6 harmonic of ϕ is still dominant like the results in Fig. 2(f). However, the amplitude of the m = 5 and m = 7 harmonics is comparable to the m = 6 harmonic for $A_{||}$, which is probably due to the kinetic effect of the thermal ions. Figure 3(f) is the radial mode structure of the parallel electric field calculated from $E_{||}^{eff} = -b_0 \cdot \nabla \phi_{eff}$ and $E_{||}^{es} = -b_0 \cdot \nabla \phi$ (Here, ϕ_{eff} and ϕ are the effective potential and the electrostatic potential, respectively.). We can see that the m = 6 harmonic of $E_{||}^{eff}$ is almost zero in the whole radial range. The m = 5 and m = 7 harmonics are finite in a wide radial range. Meanwhile, the

(a)

(b)
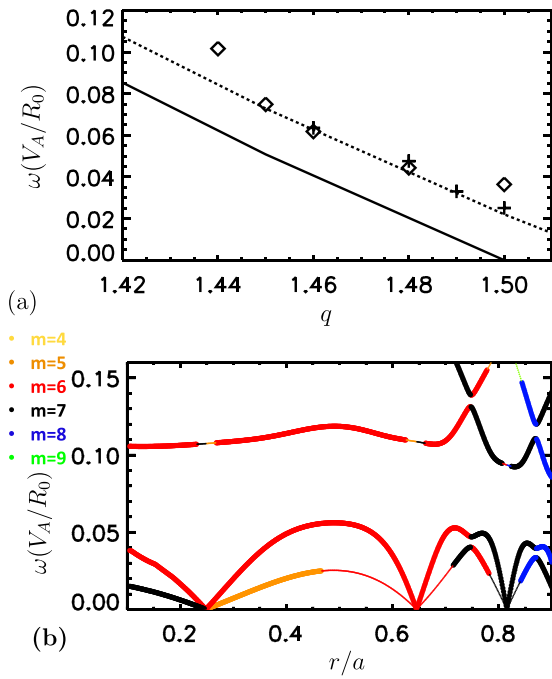
FIG. 4. Panel (a): the BAAE frequency dependent on q_{min}. Panel (b): the Alfven continuum for the $q_{min} = 1.44$ and $T_i = 0.5T_e$ case. The thick lines are the Alfven branches and the thin lines are the sound branches.

amplitude of the $E_\parallel^{es}$ harmonics is much larger than that of $E_\parallel^{eff}$, indicating that both the electrostatic potential and the vector potential contribute to the parallel electric field. The finite amplitude of the m = 5 and m = 7 harmonics in a wide

radial range also indicates that the local theory may be invalid to describe the dispersion relation of the BAAE.[7–12] Figure 3(g) shows the Alfven continuum and the BAAE frequencies. Compared with Fig. 2(h), the BAAE gap is slightly upshifted due to the higher thermal ion temperature. However, the BAAE frequency in the $T_i = 0.5T_e$ case is slightly lower than that in the $T_i = 0.02T_e$ case and locates closer to the lower boundary of the continuum. The downshift of the BAAE frequency may be due to the contributions of the kinetic effects of thermal and fast ions, which needs further investigation. Our simulation shows that the BAAE can be excited by the modest density gradient of energetic particles even when the damping rate is comparable to the real frequency.

The BAAE frequency for different q_{min} is further investigated through the excitation by the energetic particles. Figure 4(a) shows the excited BAAE frequency versus different q_{min}. We can see that the BAAE frequency decreases as q_{min} increases, which qualitatively agrees with the observation in the experiments.[9] The comparisons of the BAAE frequency between the simulation and the MHD theory are also shown in Fig. 4(a). It is found that the BAAE frequency from the GTC simulation is higher than the MHD theoretical results by $\Delta\omega = 0.022V_A/R_0$ if $k_\parallel$ is measured at q_{min} locally when calculating the MHD frequency. The BAAE frequency in the $q_{min} = 1.5$ simulations is $\omega = 0.037V_A/R_0$ for the $T_i = 0.5T_e$ simulation and is $\omega = 0.025V_A/R_0$ for the $T_i = 0.02T_e$ simulation. The higher BAAE frequency for the $T_i = 0.5T_e$ case may be due to the nonlocal mode structures

(a)

(b)

(c)

(d)
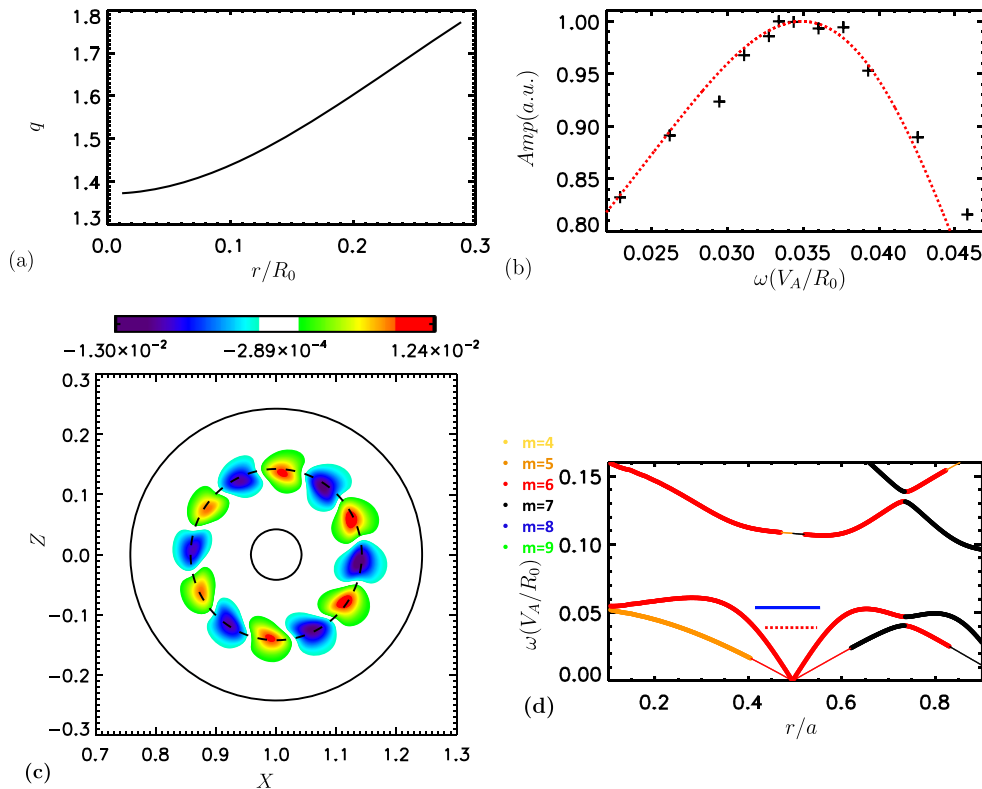
FIG. 5. Panel (a): The monotonic q profile used in the simulation. Panel (b) is the saturated mode amplitude in the antenna frequency scan. The symbols in panel (b) are the simulation results and the red dotted curve is the numerical fitting. Panel (c) is the poloidal mode structure in the energetic particle simulation. Panel (d) is the Alfven continuum. The thick lines are the Alfven branches and the thin lines are the sound branches. The horizontal lines indicate the BAAE frequency and mode width from the antenna excitation (dashed red) and energetic particle excitation (solid blue).

and the kinetic effects of the thermal and fast ions. It should be noted that the theoretical BAAE frequency is zero at $q_{min} = 1.5$ due to $k_{//} = 0$. The non-zero frequency in the GTC simulation with $q_{min} = 1.5$ indicates that the BAAE frequency is not only determined by the local parallel wave-vector. Other effects, such as radial mode structure and kinetic effects, should also be considered in determining the BAAE frequency. Moreover, it is found that the BAAE cannot be excited when $q_{min} < 1.44$ for the $T_i = 0.5T_e$ case. By investigating the Alfven continuum for the $q_{min} = 1.44$ case (Fig. 4(b)), it is found that the excited BAAE frequency is very close to the upper boundary of the BAAE gap. Since the BAAE frequency cannot be higher than the upper boundary of the BAAE gap, the BAAE does not exist when further decreasing the q_{min}. Similar effect is also found in the $T_i = 0.02T_e$ simulations where no BAAE is excited for $q_{min} < 1.46$. In the GTC simulation, it is found that the BAAE is more easily excited in the $T_i = 0.5T_e$ case than in the $T_i = 0.02T_e$ case for the same energetic particle drive although the BAAE linear damping rate is much larger in the $T_i = 0.5T_e$ case. The growth rate of the BAAE is slightly larger for the $T_i = 0.5T_e$ case even when the EP parameters, i.e., T_f, n_f, and L_{nf}, are the same for the two cases. This may be partially due to the fact that the total beta in the $T_i = 0.5T_e$ case is higher, which modifies the BAAE frequency.

B. BAAE simulation with monotonic q profile

In this section, the monotonic q profile is used with the $q = 1.5$ mode rational surface locating at the $\epsilon = 0.15$ surface (Fig. 5(a)). Other simulation parameters are the same as the reversed shear q profile simulations with $T_i = 0.5T_e$. Figure 5(b) shows the saturated BAAE amplitude in the antenna frequency scan. It is estimated that the BAAE frequency and damping rate are $\omega = 0.039V_A/R_0$ and $\gamma = -0.019V_A/R_0$, respectively. The large BAAE damping rate indicates that it is also strongly damped by the thermal ions. By using energetic particles with $T_f = 9T_e$, $n_f = 0.12n_e$, and $R/L_{nf} \approx 12$, it is found that the BAAE can be excited with frequency $\omega = 0.053V_A/R_0$ and growth rate $\gamma = 0.013V_A/R_0$. The energetic particle excited BAAE frequency is much higher than that excited by the antenna. Figure 5(c) shows the poloidal mode structure of the BAAE in the energetic particle excitation simulation. We can see that the eigenmode also has triangle structures around the $q = 1.5$ mode rational surface. However, the direction of the triangles is counter-clockwise, opposite to that in the reversed shear case shown in Figure 3(c). Figure 5(d) shows the Alfven continuum for the normal shear q profile. It is shown that a potential well is formed by the continuum around the $q = 1.5$ mode rational surface. The BAAE eigenmode resides inside this potential well.

In order to investigate whether the frequency sweeping of the BAAE also exists in the monotonic q profile, we lower the q profile slightly and excite the BAAE again with the energetic particles. It is found that the excited BAAE frequency is almost the same, i.e., no frequency sweeping. Figures 6(a) and 6(b) show the BAAE poloidal mode structure and the Alfven continuum for the case with the q profile
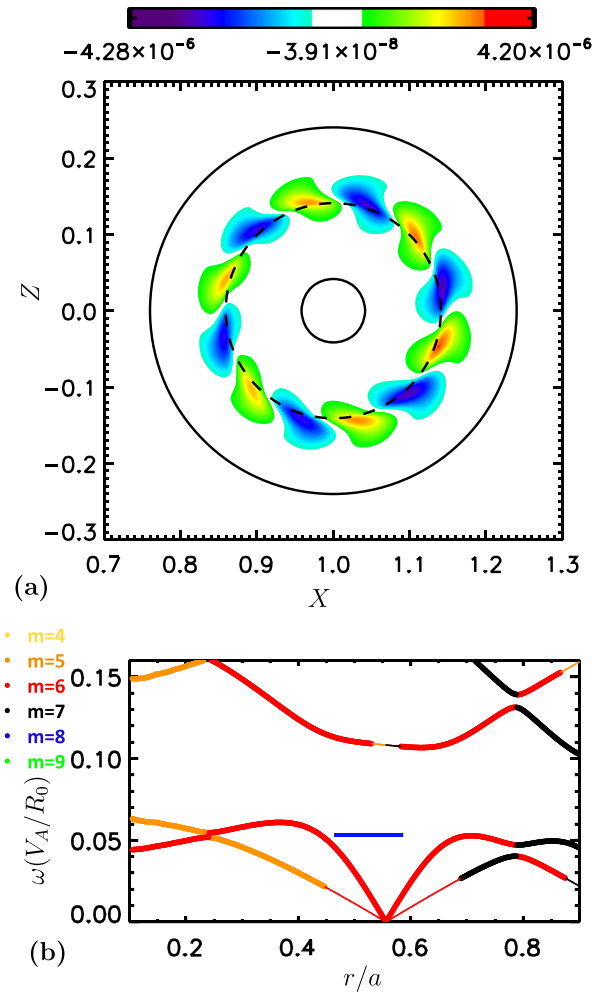
FIG. 6. Poloidal mode structure (a) and Alfven continuum (b) for the normal shear q profile shown in Fig. 5(a) but with a downshift of 0.03. The thick lines are the Alfven branches and the thin lines are the sound branches. The horizontal blue line indicates the BAAE frequency and mode width from the energetic particle excitation.

downshifted by 0.03. It is shown that the BAAE mode structure changes significantly and moves slightly outward in the radial direction. We can see that the potential well of the Alfven continuum also shifts outward from $r = 0.5a$ to $r = 0.55a$ compared with that in Fig. 5(c). This is because the slightly downshift of the q profile is almost equivalent to shifting the $q = 1.5$ mode rational surface outward in the radial direction. Therefore, the BAAE frequency is unchanged as the mode structure moves outward with the $q = 1.5$ mode rational surface.

IV. SUMMARY

In this work, the GTC is successfully used to study the beta-induced Alfven-acoustic eigenmode (BAAE) in toroidal plasmas. By using the initial perturbation, antenna excitation, and energetic particle excitation, the BAAE is verified to be weekly damped when ion temperature is much lower than electron temperature. The BAAE frequency excited by the antenna and energetic particles is almost the same as that in the initial perturbation simulation. When the ion temperature is comparable to the electron temperature, the BAAE is

found to be heavily damped by the thermal ions in the simulations of initial perturbation and antenna excitation. However, the BAAE can still be excited by the energetic particles density gradient, and the frequency is slightly higher than that estimated from the antenna excitation. The mode structure of the BAAE in the reversed magnetic shear simulation is similar to the observation in the DIII-D experiments. The frequency sweeping of the BAAE in the reversed magnetic shear simulations is consistent with the experimental observation. No frequency sweeping is found in the normal magnetic shear simulations. The triangle shape of the BAAE mode structure changes the poloidal direction in the normal magnetic shear simulations compared to that in the reversed magnetic shear simulations.

ACKNOWLEDGMENTS

[1]C. Z. Cheng, L. Chen, and M. S. Chance, Ann. Phys. **161**, 21 (1985).

[2]A. D. Turnbull, E. J. Strait, W. W. Heidbrink, M. S. Chu, H. H. Duong, J. M. Greene, L. L. Lao, T. S. Taylor, and S. J. Thompson, Phys. Fluids B **5**, 2546 (1993).

[3]W. W. Heidbrink, E. J. Strait, M. S. Chu, and A. D. Turnbull, Phys. Rev. Lett. **71**, 855 (1993).

[4]W. W. Heidbrink, E. Ruskov, E. M. Carolipio, J. Fang, M. A. Van Zeeland, and R. A. James, Phys. Plasmas **6**, 1147 (1999).

[5]H. L. Berk, D. N. Borba, B. N. Breizman, S. D. Pinches, and S. E. Sharapov, Phys. Rev. Lett. **87**, 185002 (2001).

[6]B. N. Breizman, H. L. Berk, M. S. Pekker, S. D. Pinches, and S. E. Sharapov, Phys. Plasmas **10**, 3649 (2003).

[7]N. N. Gorelenkov, H. L. Berk, E. Fredrickson, and S. E. Sharapov, Phys. Lett. A **370**, 70 (2007).

[8]N. N. Gorelenkov, H. L. Berk, N. A. Crocker, E. D. Fredrickson, S. Kaye, S. Kubota, H. Park, W. Peebles, S. A. Sabbagh, S. E. Sharapov, D. Stutmat, K. Tritz, F. M. Levinton, and H. Yuh, Plasma Phys. Controlled Fusion **49**, B371 (2007).

[9]N. N. Gorelenkov, M. A. Van Zeeland, H. L. Berk, N. A. Crocker, D. Darrow, E. Fredrickson, G. Y. Fu, W. W. Heidbrink, J. Menard, and R. Nazikian, Phys. Plasmas **16**, 056107 (2009).

[10]F. Zonca, A. Biancalani, I. Chavdarovski, L. Chen, C. D. Toria, and X. Wang, J. Phys.: Conf. Ser. **260**, 012022 (2010).

[11]D. Yu. Eremin and A. Konies, Phys. Plasmas **17**, 012108 (2010).

[12]I. Chavdarovski and F. Zonca, Phys. Plasmas **21**, 052506 (2014).

[13]Z. Lin, T. S. Hahm, W. W. Lee, W. M. Tang, and R. B. White, Science **281**, 1835 (1998).

[14]I. Holod, W. L. Zhang, Y. Xiao, and Z. Lin, Phys. Plasmas **16**, 122307 (2009).

[15]Y. Xiao, I. Holod, Z. X. Wang, Z. Lin, and T. G. Zhang, Phys. Plasmas **22**, 022516 (2015).

[16]H. S. Zhang, Z. Qiu, L. Chen, and Z. Lin, Nucl. Fusion **49**, 125009 (2009).

[17]H. S. Zhang and Z. Lin, Phys. Plasmas **17**, 072502 (2010).

[18]H. S. Zhang, Z. Lin, I. Holod, X. Wang, Y. Xiao, and W. L. Zhang, Phys. Plasmas **17**, 112505 (2010).

[19]H. S. Zhang, Z. Lin, and I. Holod, Phys. Rev. Lett. **109**, 025001 (2012).

[20]H. S. Zhang, Z. Lin, W. Deng, I. Holod, Z. X. Wang, Y. Xiao, and W. L. Zhang, Phys. Plasmas **20**, 012510 (2013).

[21]W. Deng, Z. Lin, I. Holod, Z. Wang, Y. Xiao, and H. Zhang, Nucl. Fusion **52**, 043006 (2012).

[22]W. L. Zhang, I. Holod, Z. Lin, and Y. Xiao, Phys. Plasmas **19**, 022507 (2012).

[23]Z. X. Wang, Z. Lin, I. Holod, W. W. Heidbrink, B. Tobias, M. Van Zeeland, and M. E. Austin, Phys. Rev. Lett. **111**, 145003 (2013).

[24]Z. X. Wang, Z. Lin, W. J. Deng, I. Holod, W. W. Heidbrink, Y. Xiao, H. S. Zhang, W. L. Zhang, and M. A. Van Zeeland, Phys. Plasmas **22**, 022509 (2015).

[25]C. Zhang, W. Zhang, Z. Lin, and D. Li, Phys. Plasmas **20**, 052501 (2013).

[26]J. McClenaghan, Z. Lin, I. Holod, W. Deng, and Z. Wang, Phys. Plasmas **21**, 122519 (2014).

[27]D. J. Liu, W. L. Zhang, J. McClenaghan, J. Q. Wang, and Z. Lin, Phys. Plasmas **21**, 122520 (2014).

[28]B. J. Tobias and M. A. Van Zeeland, private communication (2014).

[29]A. Fasoli, D. Borba, G. Bosia, D. J. Campbell, J. A. Dobbing, C. Gormezano, J. Jacquinot, P. Lavanchy, J. B. Lister, P. Marmillod, J.-M. Moret, A. Santagiustani, and S. Sharapov, Phys. Rev. Lett. **75**, 645 (1995).

[30]J. Harris, W. Benenson, and H. Stöcker, in *Handbook of Physics*, edited by J. Harris, W. Benenson, and H. Stöcker (Springer, New York, 2002).

[31]W. J. Deng, Z. Lin, I. Holod, X. Wang, Y. Xiao, and W. L. Zhang, Phys. Plasmas **17**, 112504 (2010).